DOI: 10.15514/ISPRAS-2019-31(6)-13

Numerical study of effect of the turbulence initial conditions on transition flow over 2D airfoil

Ali Rami, ORCID: 0000-0003-0591-6221 <ramimamdouhali@gmail.com>
N.V. Tryaskin, ORCID: 0000-0002-2208-2241 <nikita.tryaskin@smtu.ru>

State Marine Technical University (SMTU),
190121, Russia, Saint-Petersburg, Lotsmanskaya st., 3

Abstract. The performance of the airfoil is strongly dependent on the development of the boundary layer on the surface and therefore an accurate prediction of the laminar to turbulent transition onset is essential. A grid independence study is performed, turbulence variables values have been changed frequently, regularly, and carefully so that they cover the entire range of acceptable values reported by previous researches. Effects of turbulent variating at far stream on turbulent boundary layer structure and on transition stage characteristics at moderate Reynolds number $\Re = 10^6$ have been studied over a full range of angles of attack of NACA0012. numerical results have been post-processed, analyzed and found that far stream turbulence variables have a significant effect on transition characteristic, their effects on skin friction is limited to small extent along wing surface where transition take place, increasing turbulence intensity or eddy viscosity ratio at far boundary shifts transition onset towards leading edge and increase transition length.

Keyword: Turbulence intensity; Eddy viscosity ratio; k-ω SST; Transition; NACA0012

For citation: Ali Rami, Tryaskin N.V. Numerical study on effect of the turbulence initial conditions on transition flow over 2D airfoil. Trudy ISP RAN/Proc. ISP RAS, vol. 31, issue 6, 2019. pp. 203-214. DOI: 10.15514/ISPRAS-2019-31(6)-13

Численное изучение влияния начальных турбулентных параметров на переходный режим над плоским крылом

Али Рами, ORCID: 0000-0003-0591-6221 <ramimamdouhali@gmail.com>
Н.В. Тряскин, ORCID: 0000-0002-2208-2241 <nikita.tryaskin@smtu.ru>

Санкт-Петербургский государственный морской технический университет,
190121, Россия, Санкт-Петербург, ул. Лоцманская, 3

Аннотация. Эксплуатационные характеристики аэродинамического профиля сильно зависят от развития пограничного слоя на поверхности, и поэтому точный прогноз начала ламинарного перехода к турбулентному имеет важное значение. Проводится исследование сеточной сходимости, начальные значения турбулентных параметров меняются таким образом, чтобы охватить весь диапазон допустимых значений. Влияние параметров турбулентности в дальнем потоке на структуру турбулентного пограничного слоя и на характеристики зоны ламинарно-турбулентного перехода при умеренном числе Рейнольдса $\Re = 10^6$ было изучено во всем диапазоне углов атаки NACA0012. Численные результаты были проанализированы и обнаружено, что переменные турбулентности в дальнем потоке оказывают существенное влияние на характеристики перехода, их влияние на изменение коэффициента трения ограничивается областью крыла, где происходит переход. При увеличении интенсивности турбулентности или коэффициента вихревой вязкости на дальней границе сдвигается начало перехода к передней кромке и увеличивается его длина.

Ключевые слова: интенсивность турбулентности; коэффициент вихревой вязкости;, k-ω SST; ламинарно-турбулентный переход, NACA001.

Для цитирования: Али Рами, Тряскин Н.В. Численное изучение влияния начальных турбулентных параметров на переходный режим над плоским крылом. Труды ИСП РАН, том 31, вып. 6, 2019 г., стр. 203–214 (на английском языке). DOI: 10.15514/ISPRAS–2019–31(6)–13

1. Introduction

Flows at moderate and high Reynolds number are characterized by complex turbulent boundary-layer effects, including leading-edge laminar-to-turbulent transition, flow reattachment, trailing-edge separation, and leading-edge separation.

Laminar-to-turbulent transition in shear layer of the flows over airfoil is of particular importance, although it has subjected to intensive research over the past decades but it still far from completely understood.

The location where transition starts, and the spatial extension occupied by it are of a great importance in the airfoil performance. Therefore, the accurate understanding of transition process allows us adjusting the flow and controlling its nature so we can delay the turbulent phase where laminar flow characteristics are desirable or to accelerate it where high mixing rates of turbulent flow are of interest.

The difficulty in modelling transition arises from its non-linearity, wide range of scales, and the fact that it can occur through different mechanisms [1]. An overview of different scenarios of laminar-turbulent transition can be found in studies [2,3,4].

The transition process is greatly influenced by pressure gradients and separation, Mach number effects, free-stream turbulence, wall roughness, streamline curvature, surface heating or cooling, suction or blowing of fluid from the wall and so on [5].

H.A. Madsen et al. researched effects of leading-edge roughness on Laminar-Turbulent Transition, their analyses show that the critical height of the leading-edge roughness is to be met in order to have a bypass transition to turbulent flow [6]. Mayle [7] ensured the importance of pressure gradient and turbulence intensity on the transition onset on airfoil. Butler et al. [8] studied effects of turbulent intensity on flow separation at low Reynolds number and found that increasing turbulence intensity to high level 10% prevent the separation. Mueller and Pohlen [9], Hoffmann [10] and Huang and Lee [11] show that the increasing in turbulent intensity has resulted increase in maximum lift coefficient for the airfoil. Jian-Ping Wang et al researched the effect of the turbulence intensity of the oncoming flow with low Reynolds numbers on the airfoil performance and found that turbulence intensity has significant impact on lift and drag coefficients [12]. Ning Cao focused in his study on the independent effects of the turbulence intensity and integral length scale on the Cl and Cd, of an asymmetric, high lift airfoil, at different $\Re$ and found that increasing Tu leads to delay stall at high angle of attack [13],

However, a literature review shows that there is a little investigation about the effects of eddy viscosity ratio at certain value of turbulent intensity on the transition character over airfoil at moderate Reynold number. Bridging this gap is the main motivation of current study. So, this paper deals with the effects of far stream turbulence variables on the onset and length of laminar to turbulent transition and its influence on flow character and airfoil performance at moderate Reynold number.

The paper starts with a description of the methodology in section 2, which includes a brief description of used turbulence model k-ω SST and wall functions, the geometrical and operational characteristics of the chosen airfoil, the grid and computational domain, the numerical settings and grid convergence analyze which include a sensitivity analyze of results to grid resolution and in addition to validation with experimental data [14].

Finally results and discussion of far stream turbulence parameter effects on transition onset and length are discussed in section 3, conclusions are presented in section 4.

2. Methodology

2.1 k-ω SST standard turbulence model

The Menter Shear Stress Transport Turbulence Model k-ω SST is a two-equation eddy-viscosity model used for many hydrodynamic and aerodynamic applications, this model combines the well-known low Reynolds turbulence model $k-\omega$ and high Reynolds turbulence model $k-\varepsilon$, the former is suitable for simulating flow in the viscous sub-layer but it suffers from a high sensitivity to the inlet free-stream turbulence properties, while the latter is ideal for predicting flow behavior in regions away from the wall but it performs poorly in adverse pressure gradient situations and cannot be used all the way down to wall.

To eliminate the disadvantages of each individual model and to maintain their strengths a blinder function F_1 is used to switch between $k-\varepsilon$ in the free stream and $k-\omega$ near the walls, which ensures that the appropriate model is utilized throughout the flow field. Therefore, k-ω SST model can be used all the way down to the wall without being influenced by free-stream turbulence [15,16].

The two transport equations that form the basis of the model are as follows:

$$\frac{\partial(\rho k)}{\partial t}+\frac{\partial\left(\rho u_j k\right)}{\partial x_j}=P-\beta^*\rho\omega k+\frac{\partial}{\partial x_j}\left[(\mu+\sigma_k\mu_t)\frac{\partial k}{\partial x_j}\right]$$

$$\frac{\partial(\rho\omega)}{\partial t}+\frac{\partial\left(\rho u_j\omega\right)}{\partial x_j}=\frac{\gamma}{\nu_t}P-\beta\rho\omega^2+\frac{\partial}{\partial x_j}\left[(\mu+\sigma_\omega\mu_t)\frac{\partial\omega}{\partial x_j}\right]+2(1-F_1)\frac{\rho\sigma_{\omega2}}{\omega}\frac{\partial k}{\partial x_j}\frac{\partial\omega}{\partial x_j}$$

In these equations, P is the sources term, F_1 is a blending function and β, β^*, $\sigma_{\omega2}$, σ_ω and σ_k are constant.

Viscous effects near walls are characterized by the non-dimensional wall distance $y^+=(y\cdot u^*)/\nu$, where u^* is the friction velocity, y is the distance to the wall, and ν is the kinematic viscosity of the fluid. Using low Reynolds turbulence model as approach to simulate flow near the wall enforces us to place the first cell center in the viscous sublayer, advised to be $y^+\approx 1$, that leads to finest mesh and thus increasing computing time, the case will be the same when using modified high Reynolds turbulence models. Launder and Spalding [17] proposed the wall function which is an empirical equation used to satisfy the physics of the flow in the near wall region so the first cell center now needs to be placed in the log-law region $y^+\geq 30$ to ensure the accuracy of the result, both approaches produce large errors if used outside of their range of validity.

It is difficult to ensure that cells adjacent to the wall will all fall within the desired layer, so in OpenFOAM the existing wall functions have been modified and improved to include the buffer layer [18] and to ensure that they can provide the accurate result so wherever the position of the first cell center [19]. In this study we will employ OpenFOAM Low Reynold wall functions to approximate the viscous quantities in the boundary layer surrounding the airfoil, this type of wall functions has improved to allow the first cell center to be placed in buffer layer, depending on internal switch developed based on the value of yPlusLam coefficient. yPlusLam is determined by an iteration process designed to divide buffer layer into two parties, one uses the liner relation as that in viscous sublayer, and the other uses logarithmic function as that in logarithmic region. So, these wall functions give appropriate values wherever the position of the first cell center, that gives us more flexibility during the mesh optimization stage, facilitate calculations and reduce simulation time, now minimum wall distance y and y^+ value could be enlarged, and the case will be properly modeled [19].

We have to indicate that the theory of wall functions used in OpenFOAM is based on the paper proposed by Georgi Kalitzin et al. [20].

2.2 Chosen Airfoil

In this paper we will use NACA 0012 airfoil, a conventional, symmetrical airfoil with maximum thickness $12\%C$ located at $30\%C$, where C is the airfoil chord length.

NACA 0012 belongs to NACA 4-digits airfoil series (NACA MPXX), a series controlled by 4 digits prepared carefully to describe the geometrical properties of an airfoil, maximum camber, position of the maximum camber and maximum airfoil thickness at $30\,\%$ chord, respectively. These digits are given as percentages of the airfoil chord length C. The camber line of airfoil, in addition to the perpendicular distribution of the thicknesses along its length, is given by mathematical equations, thus facilitate the generation of the geometrical section of any airfoil.

2.3 Computational domain and grid

O-Grid domain prepared to simulate flow over the wing, based on similar studies and to avoid confinement effects and consequently to apply the far-field boundary, the circular domain surrounding the airfoil of unit chord was chosen to be of radius $50C$, fig. 1(a).

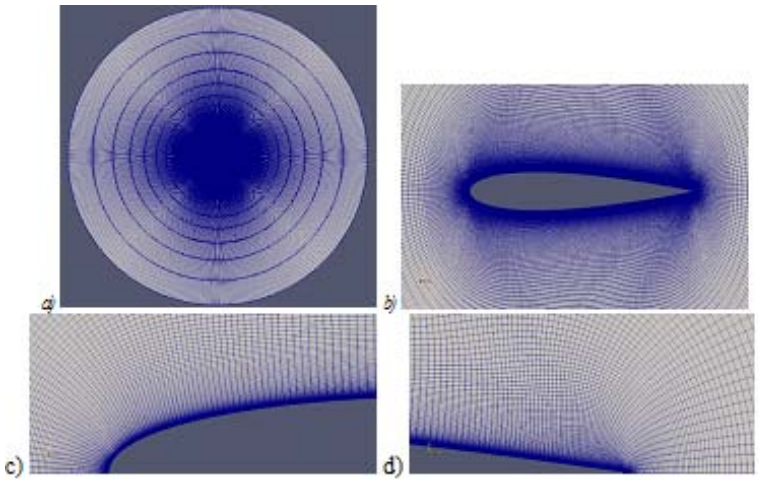

Fig. 1 (a) O-Grid computational domain mesh; (b) Internal domain mesh; (c) Leading edge spans; (d) Trailing edge spans

To improve the accuracy of the results and to reduce the consumed time, O-Grid approach is used to generate a 2-D multi zone structured mesh, the resulted mesh is divided depending on its discretization density into two different zones, fine and coarse mesh.

Fine mesh forms the internal zone of the computational domain, extends along a distance of $0.3C$ perpendicularly to airfoil connectors with a growth rate of 1.01, so the mesh is fine next to wing and relatively coarser far away fig. 1(b). Benefiting from Open Foam improved wall functions, and to achieve a balance between computation speed and accurately capturing the linear viscous sublayer, the minimum wall normal distance is maintained to be 0.0001 and therefore maximum y^+ values of the simulations at various angle of attack will be in the order of $y^+<10$.

Airfoil connectors were divided into 405 points. To improve aspect ratio as well as mesh distribution around the wing, taking into consideration the selected values of growth rate and wall distance, the leading and trailing edge spans were chosen to be identical as 0.0001, as shown in fig. 1(c),(d).

The second zone is a coarser mesh, encloses the internal zone with a growth rate of 1.3 normal to airfoil connectors, its minimum first cell high was chosen carefully to ensure mesh continuity and to avoid, as much as possible, solver convergence errors.

It is believed that the selected growth rate ratio, coupled with the first cell high and edges span are convenient to make mesh fine enough in vicinity of airfoil, and to solve the flow well around it. The selected values consider the conditions of the physical phenomena we simulate $\Re = 10^6$, in addition to the modeling software and boundary conditions we plan to use.

2.4 Numerical settings

The open-source CFD software package OPENFOAM was chosen to solve the incompressible Reynolds-averaged Navier-Stokes (RANS) equations. being an open-source package, having a wide variety of boundary-conditions, wall-functions, finite volume solution and schemes gives it a great advantage of managing, controlling and detecting the whole simulation processes. all the simulation settings were set corresponding to the characters and circumstances of the experiment [14].

SIMPLE, a pressure-velocity coupling algorithm based on finite volume method was used. Turbulence is modeled using the 2-equation transition turbulence model K-ω SST and the discretization of turbulence model equations was made using the upwind second order scheme, in order to obtain high accuracy, the convergence criterion is set at $1 \cdot 10^{-6}$.

according to the environment of the experimental work, the free stream temperature is $293.15K$, therefore the corresponding value of fluid kinematic viscosity ν is set to $1.516 \cdot 10^{-5}$.

The consistent boundary conditions, freestreamPressure and freestreamVelocity, were used simultaneously to give appropriate condition for pressure and speed at far stream based on the velocity orientation. At far stream, atmospheric pressure of uniform value 0 is applied, Reynolds number used in experiments has a value of $\Re = 10^6$, so the free-stream velocity (U_∞) is set to constant uniform value of (15.16,0,0) m/s and its components for different angles of attack α are calculated by simple formulas $V_x = V \cdot cos(\alpha)$, $V_y = V \cdot sin(\alpha)$. zeroGradient and no-Slip conditions are applied to pressure and velocity along the airfoil surface respectively. lowReWallFunction was used for k and ν_t while omegaWallFunction was used for ω.

The turbulence intensity Tu and eddy viscosity ratio μ_t/μ have been set at the inlet to 0.1% and 0.01 respectively, which give the kinematic turbulent energy k and turbulent dissipation ω at far-stream boundary a value of $0.0003447[J/kg]$, $2274[1/s]$ respectively, during the simulation operation their values have been systematically changed. Turbulence length scale has remained constant $136 \cdot 10^{-7}[m]$ and was not changed for all tested cases since its variation has not any considered effects on final results [21,22].

2.5 Grid convergence analysis

To investigate the discretization errors and to validate the dependency of simulation results on the computational grid, the simulation was performed on a series of three levels of successively finer grids, a coarse, medium and fine mesh.

In order to distinguish the discretization error from iterative convergence and computer rounding errors the grid refinement ratio in x direction selected to be of $r = 2$, on other hand this allows the Grid Convergence Index (GCI) to be employed [23,24,25]. hence the number of nodes along the whole airfoil surface would be 200, 400 and 800 nodes respectively, the drag coefficient C_d, the most sensitive variable [27], at $\alpha = 0°$ and $\alpha = 8°$ was set as the criterion for mesh dependency.

A grid convergence was performed, the order of grid convergence P was calculated and found to be of second-order $P = 1.82 \approx 2$ which is close to the theoretical order of convergence. The reduction of the discretization error as a function of grid size is shown in fig. 2. Richardson's

extrapolation spatial convergence of CFD simulation was performed on the finest two grids to predict the true value of the drag coefficient at zero-grid spacing based on order of convergence, and found to be 0.01 (see table 1). The grid convergence indexes GCI for fine-medium grid and medium-coarse grid were calculated using a safety factor for three grids $fs = 1.25$ and found that $GCI_{12} = 0.146$, $GCI_{23} = 0.521$ and they achieve the relation $GCI_{23}/(r^p \cdot GCI_{12}) = 1.003$ which is approximately one, and indicates that we are asymptotically approaching a converged answer, and thus our solution is definitely grid independent (see table 1).

Table 1. Studying the Computational grid convergence for drag coefficient at $\alpha = 0°, 8°$

Angle of Attack	fine mesh	medium mesh	coarse mesh	Order of Grid Convergence P
0	0.010281	0.010250	0.010142	1.824499
8	0.015261	0.015087	0.014468	1.822492
Richardson extrapolation	$GCI_{12}\%$	$GCI_{23}\%$	$\frac{GCI_{23}}{(r^p \bullet GCI}$	Richardson extrapolation
0.010293	0.146650	0.520965	1.002991	0.010293
0.015330	0.564287	2.018959	1.011585	0.015330

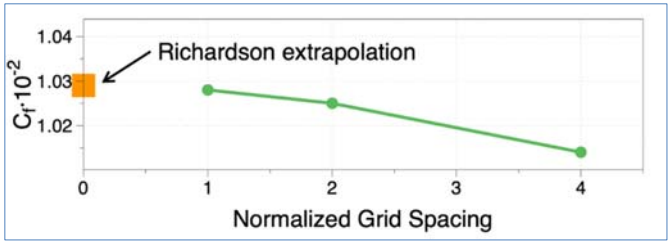

Fig. 2. Grid convergence study

Furthermore, the drag coefficient C_d, the most sensitive variable [26], and lift coefficients (C_l) of the airfoil at moderate Reynold number are compared for the three grids in order to further investigate the grid dependence of the results (see fig. 3). It can clearly be seen that the ability of predicting increases as mesh size increases:

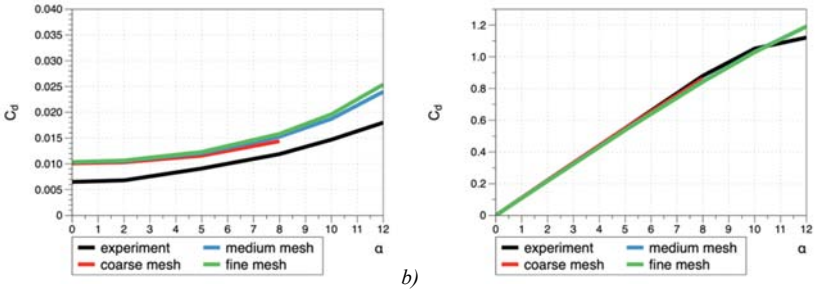

a) *b)*

Fig. 3. Drag and lift curves for the three grids (coarse, medium, fine.

The maximum absolute difference is 0.0004 at $\alpha = 8°$ which results in less than 3% difference in drag coefficient. The difference which can be observed can be attributed to a slight improvement in the prediction of flow separation on the airfoil which also has a very limited effect on the airfoil behavior.

Based on these results the medium grid was selected for the rest of the calculations, and it is believed that the initial 400 nodes grid was quite enough to capture the flow.

3. Results and discussion

The onset of the transition phase is evidenced by the apparent changes in the behavior of skin-friction curve C_f. The minimum local value in the friction curve indicates the start of the transition phase, the emergence of bubbles of turbulence, its growth in the laminar layer, its explosion and subsequent fusion, thus announcing manifestation of the fully developed turbulent flow.

The huge computational possibilities and vast computing resources available at laboratories of SMTU university allowed conducting a digital modeling and simulation of flow around 2-D NACA0012 profile. The simulations were done for a series of far-stream turbulence intensities and eddy viscosity ratios to indicate their effects on the onset and length of transition phase for airfoil located in viscous incompressible fluid, viscosity $\nu = 1.516$ at temperature $293.15K$, at various angle of attack and constant $\Re = 10^6$.

3.1 Effects of eddy viscosity ratio on onset and length of transition over the airfoil

Studying the effects of eddy viscosity ratio can be done by examine the behavior of skin friction coefficient curve at different value of μ_t/μ. Generally, μ_t/μ has a local effect on the skin friction coefficient (C_f), which maintains itself along the length of the wing, except for a very limited area of the wing surface along it the transition process take place. Using higher values for μ_t/μ at the far boundary increases the value of skin friction coefficient (C_f) in this area, as well as shifting the onset transition point towards the front edge of the wing.

Fig. 4(a) shows the curves of the skin friction coefficient variation along a section of a two-dimensional airfoil NACS0012 located at angle of attack $\alpha = 0°$ in a non-compressible viscous flow field at turbulence intensity $Tu = 0.1$ and various values of μ_t/μ.

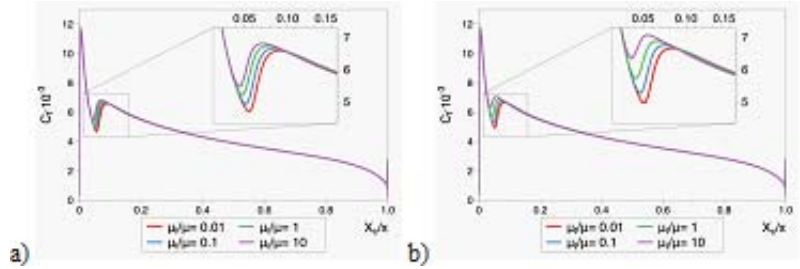

Fig. 4. Skin friction coefficient curves on NACA0012 surface at angle of attack 0 Degree, for various values of far-stream turbulence variables:
a) Tu=0.1, b) Tu=6

The curves of fig. 4(a) show that increasing the Eddy viscosity ratio at a certain value of Turbulence intensity leads to shift onset transition location towards leading edge of the airfoil. At a low value of far stream turbulence intensity $Tu = 0.1$, increasing μ_t/μ from 0.01 to 10 at moderate values of Reynolds number $\Re = 10^6$ leads to shift the transition point of flow over NASA 0012 surface towards leading edge from 0.0558 to 0.04387, which represents a change of $1.19\,\%$ of chord length. This displacement is accompanied by an increase in the value of skin friction coefficient from $4.681 \cdot 10^{-3}$ to $5.457 \cdot 10^{-3}$, a relative increase of $16.57\,\%$, and a decrease in the length of the transition.

To investigate generalization of the reported conclusions, the simulation was repeated at higher value of far stream turbulence intensity, $Tu = 6$. The resulted skin friction coefficients at different values of eddy viscosity ratio were plotted on the right side. The curves of fig. 4(b) ensure that C_f curves maintain its behavior at high values of turbulence intensity too, except that the effect of μ_t/μ is more pronounced, this means that the ability of μ_t/μ to influence the skin friction coefficient is improved with the increase in the turbulence intensity, at higher disturbance values, the same increase in μ_t/μ causes a greater increase in the friction coefficient. Curves of Figure 6,b at $Tu = 6$ confirm that an increase in μ_t/μ value from 0.01 to 10 leads to shifting the transition point from 0.0556 to 0.0409694, which represents a change of $1.46\,\%$ of the airfoil chord. This change in practice is $0.27\,\%$ higher than using the low value of the turbulence intensity $Tu = 0.1$ at far boundary. The increase in μ_t/μ from 0.01 to 10 leads to an increase of C_f from $4.69702 \cdot 10^{-3}$ to $5.71491 \cdot 10^{-3}$ which constitutes $21.67\,\%$ of the value of the friction coefficient. If compared with the value of the change at small values of turbulence intensity $Tu = 0.1$, we will find that this increase is $5.1\,\%$

3.2 Effect of turbulence intensity on onset and length of transition over the airfoil

Skin friction coefficient at certain value of eddy viscosity ratio were plotted for different values of turbulent intensity, see fig. 5.

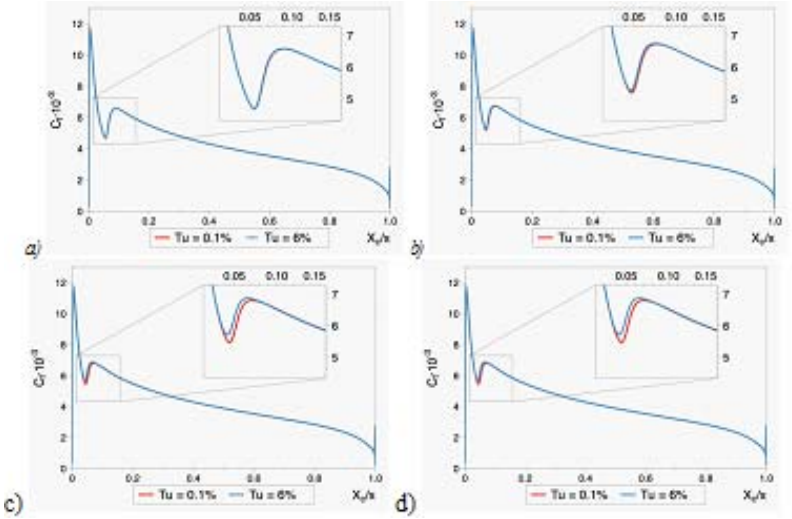

Fig. 5. Skin friction coefficient curves on NACA0012 surface at angle of attack 0 Degree, at certain value of eddy viscosity ratio and different values of far-stream turbulence intensity:
a) μ_t/μ=0.01, b) μ_t/μ=0.1, c) μ_t/μ=1, d) μ_t/μ=10

Analysis of shape curves indicates that increased intensity of turbulence slightly excites the layer instability over the airfoil surface and therefore increases the rates of disturbance in the sheer layer causing upstream shift of transition onset as well as slightly increase in transition length.

Despite the values of turbulence intensity Tu vary widely at boundaries, their values next to the wing are convergent and the modeling values of the transition onset are therefore close to each other. This behavior is related to the ability of the grid to solve decay equations at different values of turbulence variables. When high values are used at boundary, the decay rates modeled by grid are dramatically decreased while gradually decreased when low values are used.

3.3 Effects of angle of attack on onset and length of transition over the airfoil.

To study angle of attack effects on the characteristics of the transition phase, the previous simulation was repeated at the same values of far stream turbulence intensity and eddy viscosity ratios but using different values for angle of attack.

Curves of fig. 6, 7 illustrate the variation of the skin friction coefficient along a section of a two-dimensional airfoil NACS0012 located at angle of attack $\alpha = 8°$,$\alpha = 10°$, respectively, immersed in a non-compressible viscous flow field at far stream turbulence intensity $Tu = 0.1$ (left side), and $Tu = 6$ (right side) for various values of μ_t/μ.

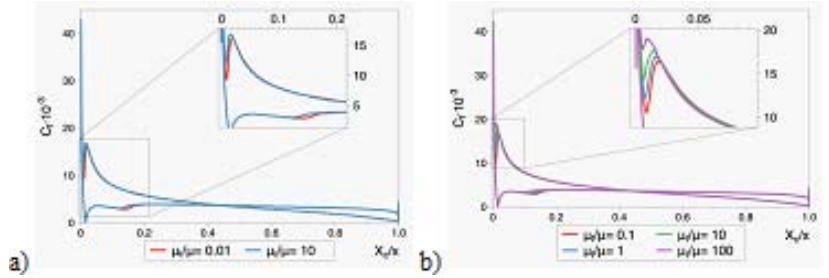

Fig. 6. Skin friction coefficient curves on NACA0012 surface at angle of attack 8 Degree, for various values of far-stream turbulence variables:

a) Tu=0.1, b) Tu=6

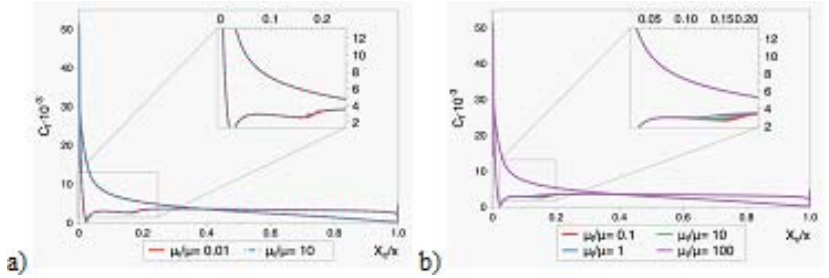

Fig. 7. Skin friction coefficient curves on NACA0012 surface at angle of attack 10 Degree, for various values of far-stream turbulence variables:
a) $Tu = 0.1$, b) $Tu = 6$

By comparing the curves of the fig. 4, 6, and 7 at the corresponding values of the turbulence intensity, we observe that skin friction coefficient curves maintain their behavior at the various values of angle of attack, but as angle of attack increases the effects of μ_t/μ on the transition onset point fades. Curves indicate that although the μ_t/μ is increased from 0.01 to 100, the transition start at approximately the same point, which in turn shifts towards the leading edge of the wing as angle of attack increases.

During numerical simulation process, it was observed that the simultaneous use of small values for Tu with large values for μ_t/μ causes convergence problems, which explain absence of some skin friction coefficients curves at $Tu = 0.1$ from results of different angle of attack.

Reviewing previous figures indicates that increasing angle of attack requires increase in Tu values to overcome convergence problems which occur at low values of Tu at the same angle.

Finally, we should point out that the super-fining of the grid cause losing its sensitivity to changes in the disturbance variables at far boundaries, so that the turbulent model k-w SST cannot predict the transition point. Fig. 8 shows simulated skin friction coefficient on super fine mesh at different angle of attack and various values of far stream turbulence variables.

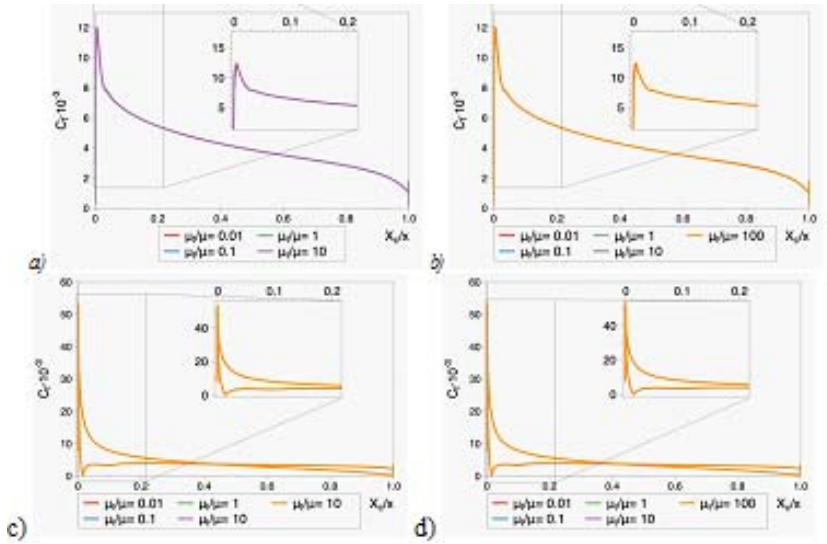

Fig. 8. Skin friction coefficient curves on NACA0012 surface simulated on super-fining grid at different angle of attack, for various values of far-stream turbulence variables:
a) $\alpha = 0°$, $Tu = 0.1$, b) $\alpha = 0°$, $Tu = 6$, c) $\alpha = 8°$, $Tu = 0.1$, d) $\alpha = 8°$, $Tu = 6$

4. Conclusions

RANS Simulations were carried out on a NACA0012 airfoil using the software OpenFoam and turbulent model k-ω SST in order to study effects of turbulence variables at far stream on transition flow characters over the airfoil at moderate Reynolds number of $\Re = 10^6$. Analyses and numerical investigation leads to the following conclusions.

- Far stream turbulence variables have significant effects on transition flow character over airfoil at moderate Reynolds number.
- Effect of turbulence intensity and eddy viscosity ratio at far stream on the skin friction coefficient is negligible, except for a limited area where the transition occurs.
- Using high values for Tu gives a greater ability to control the desired position of the transition phase on the wing surface, which is done by changing the μ_t/μ on a wide range from 0.01 to 100 without convergence problems.
- Using small values for Tu causes convergence problems especially if used with large values of μ_t/μ which in turn limits the controlling ability.
- Increasing Tu shifts the transition onset a little towards the leading edge and has a negligible effect on transition length and skin friction coefficient at transition phase.
- Increasing μ_t/μ shifts the transition onset towards the leading edge, as well as increases skin friction coefficient at transition phase, increases transition length.
- Increasing angle of attack reduces sensitivity to changes in far stream turbulence variables.

- Increasing angle of attack requires simultaneous increase in turbulence intensity at far stream, so solver reaches a stable solution without convergence problems over a wide range of μ_t/μ values.
- Over-fining of the computational domain causes grid to lose its sensitivity to changes in disturbance values at far boundaries.

References / Список литературы

[1]. Rui Miguel Alves Lopes. Calculation of the flow around hydrofoils at moderate Reynolds numbers. Master thesis. Instituto Superior Tecnico, Lisboa, Portugal, 2015.

[2]. Robert Edward Mayle. The Role of Laminar-Turbulent Transition in Gas Turbine Engines. ASME Journal of Turbomachinery, vol. 113, no. 4, 1991, pp. 509-537.

[3]. Emmons H.W. The laminar-turbulent transition in a boundary layer. Part I. Journal of the Aeronautical Sciences, vol. 18, 1951, pp. 490-498.

[4]. Robin Blair Langtry. A correlation-based transition model using local variables for unstructured parallelized CFD codes. PhD Thesis, Universität Stuttgart, Fakultät Maschinenbau, 2006.

[5]. F.R. Menter, R.B. Langtry, S.R. Likki, Y.B. Suzen, P.G. Huang, S. Völker. A Correlation-Based Transition Model Using Local Variables – Part I: Model Formulation. ASME Journal of Turbomachinery, vol. 128, no. 3, 2006, pp. 413-422.

[6]. Ö.S. Özçakmak, H.A. Madsen, N.N. Sørensen, J.N. Sørensen, Andreas Fischer, C. Bak. Inflow Turbulence and Leading Edge Roughness Effects on Laminar-Turbulent Transition on NACA 63-418 Airfoil. Journal of Physics: Conference Series, vol. 1037, issue 2, 2018, article no. 022005.

[7]. R.E. Mayle. The Role of Laminar-Turbulent Transition in Gas Turbine Engines. ASME Journal of Turbomachinery, vol. 113, no. 4, 1991, pp. 509-537

[8]. Butler R.J., Byerley A.R., VanTreuren K., and Baughn J.W. The Effect of Turbulence Intensity and Length scale on Low-pressure Turbine Blade Aerodynamics. International Journal of Heat and Fluid Flow, vol. 22, issue 2, 2001, pp. 123-133.

[9]. Mueller T.J., Pohlen L.J. The Influence of Free-Stream Disturbances on Low Reynolds Number Airfoil Experiments. Experiments in Fluids, vol. 1, issue 1, 1983, pp 3–14.

[10]. Hoffmann J.A. Effects of Freestream Turbulence on the Performance Characteristics of an Airfoil. AIAA Journal, vol. 29, no. 9, 1991, pp. 1353-1354.

[11]. Huang R.F. and Lee H.W. Effects of Freestream Turbulence on Wing-Surface Flow and Aerodynamic Performance. Journal of Aircraft, vol. 36, no. 6, 1999, pp. 965-972.

[12]. Shao-wu Li, Shu Wang, Jian-ping Wang, Jian-chun Mi. Effect of turbulence intensity on airfoil flow: Numerical simulations and experimental measurements. Applied Mathematics and Mechanics, vol. 32, 2011, pp. 1029-1038.

[13]. Cao Ning. Effects of turbulence intensity and integral length scale on an asymmetric airfoil at low Reynolds numbers. Master Thesis. University of Windsor, Canada, 2010.

[14]. Sheldahl R.E. and Klimas P.C. Aerodynamic characteristics of seven symmetrical airfoil sections through 180-degree angle of attack for use in aerodynamic analysis of vertical axis wind turbines. Technical Report, U.S. Department of Energy, Office of Scientific and Technical Information, 1981.

[15]. Menter F.R., Kuntz M., Langtry R. Ten Years of Industrial Experience with the SST Turbulence model. In Proc. of the Fourth International Symposium on Turbulence, Heat and Mass Transfer, 2003, pp. 624 – 632.

[16]. Daniel Lindblad. Implementation and run-time mesh refinement for the k−ω SST DES turbulence model when applied to airfoils. Project work. Chalmers University of Technology, 2014.

[17]. D.B. Spalding. A single formula for the “law of the wall”. Journal of Applied Mechanics, vol. 28, issue 3, 1961, pp. 455-458.

[18]. Liu S.N. Implementation of a Complete Wall Function for the Standard k-ε Turbulence Model in OpenFOAM 4.0. Technical report. Chalmers University of Technology, 2016.

[19]. Fangqing Liu.: A Thorough Description of How Wall Functions are Implemented in OpenFOAM. Technical report. Chalmers University of Technology, 2016.

[20]. Georgi Kalitzin, Gorazd Medic, Gianluca Iaccarino, Paul Durbin. Near-wall behavior of rans turbulence models and implications for wall functions. Journal of Computational Physics, vol. 204, issue 1, 2005, pp. 265–291.

[21]. Robert J. Butler, Aaron R. Byerley, Kenneth VanTreuren, James W. Baughn. The effect of turbulence intensity and length scale on low-pressure turbine blade aerodynamics. International Journal of Heat and Fluid Flow, vol. 22, issue 2, 2001, pp. 123-133.

[22]. Cao Ning. Effects of turbulence intensity and integral length scale on an asymmetric airfoil at low Reynolds numbers. Master thesis. University of Windsor, Canada, 2010.

[23]. Roache P.J. Perspective: A Method for Uniform Reporting of Grid Refinement Studies. Journal of Fluids Engineering. Journal of Fluids Engineering, vol. 116, no. 3, 1994, pp. 405-413.

[24]. Roache P.J. Quantification of Uncertainty in Computational Fluid Dynamics. Annual Review of Fluid Mechanics, vol. 29, 1997, pp. 123-160.

[25]. Ali Rami, Tryaskin N.V. Effects of turbulence variables on transition flow characteristics over NACA0012 airfoil. Marine intellectual technologies. № 3(45), vol. 2, 2019, pp. 39-44 (in Russian) / Али Рами, Тряскин Н.В. Влияние параметров турбулентности на характеристики переходного режима течения при обтекании профиля NACA 0012. Морские интеллектуальные технологии. № 3(45), том 2, 2019 г., стр. 39-44.

[26]. F. R. Menter, M. Kuntz, and R. Langtry. Ten Years of Industrial Experience with the SST Turbulence Model. In Proc. of the 4th International Symposium on Turbulence, Heat and Mass Transfer, 2003, pp. 625-632.

Информация об авторах / Information about authors

Рами АЛИ – аспирант кафедры гидроаэромеханики и морской акустики. Научные интересы: численное моделирование, интенсивность турбулентности, уравнения Рейнольдса.

Rami ALI is a PhD student of the Department of Hydroaeromechanics and Marine Acoustics. Research interests: numerical modeling, turbulence intensity, Reynolds equations.

Никита Владимирович ТРЯСКИН – кандидат технических наук, доцент кафедры гидроаэромеханики и морской акустики. Научные интересы: гидродинамика, турбулентность, уравнения Рейнольдса, численное моделирование.

Nikita Vladimirovich TRYASKIN – candidate of technical sciences, associate professor of the Department of Hydroaeromechanics and Marine Acoustics. Research interests: hydrodynamics, turbulence, Reynolds equations, numerical simulation.